Article

Not peer-reviewed version

Polymer Biocompositions and Hybrid Polymer Nanobiocomposites Based on P3HB with an Aliphatic Polyurethane and Organically Modified Montmorillonite

Beata Krzykowska *, Anna Czerniecka-Kubicka, Anita Białkowska, Mohamed Bakar, Karol Hęclik, Lucjan Dobrowolski, Michał Longosz, Iwona Zarzyka *

Posted Date: 31 October 2023

doi: 10.20944/preprints202310.2030.v1

Keywords: polyhydroxyalkanoates; poly(3-hydroxybutyrate); composites; nanocomposites; structure-properties relationship

Article

Polymer Biocompositions and Hybrid Polymer Nanobiocomposites Based on P3HB with an Aliphatic Polyurethane and Organically Modified Montmorillonite

Beata Krzykowska [a),*], Anna Czerniecka-Kubicka [b)], Anita Białkowska [c)], Mohamed Bakar [c)], Karol Hęclik [d)], Lucjan Dobrowolski [d)], Michał Longosz [a)] and Iwona Zarzyka [a),*]

[a)] Department of Organic Chemistry, Faculty of Chemistry, Rzeszów University of Technology, Powstańców Warszawy 6, 35-959 Rzeszów, Poland, b.krzykowska@prz.edu.pl
[b)] Department of Experimental and Clinical Pharmacology, Medical College of Rzeszow University, The University of Rzeszow, 35-310, Rzeszow, Poland; aczerniecka@ur.edu.pl
[c)] Faculty of Chemical Engineering and Commodity Science, University of Technology and Humanities, Chrobrego 27, 26-600 Radom, Poland; a.bialkowska@uthrad.pl, m.bakar@wp.pl
[d)] Department of Biotechnology and Bioinformatic, Faculty of Chemistry, Rzeszów University of Technology, Powstańców Warszawy 6, 35-959 Rzeszów, Poland; kheclik@prz.edu.pl; ldobrowolski@prz.edu.pl
* Correspondence: Beata Krzykowska, b.krzykowska@prz.edu.pl, Iwona Zarzyka, izarzyka@prz.edu.pl, tel. +480178651762, fax. +480178543655

Abstract: Due to the growing interest in biopolymers, biosynthesizable and biodegradable polymers currently occupy a special place. Unfortunately, the properties of native biopolymers are not satisfactory, which explain that attempts are being made to modify them. The work attempts to improve the properties of poly(3-hydroxybutyrate) (P3HB) using linear aliphatic polyurethane (PU) based on 1,4-butanediol and hexamethylene 1,6-diisocyanate. The conducted studies on the effect of the amount of PU used (5, 10, 15 and 20 wt.%) showed an improvement in the thermal properties of the prepared polymer blends. There was an increase in the degradation temperature of the obtained blends in relation to the native P3HB by 12-57°C, and the difference between the melting point and the degradation point was above 100°C for most of the obtained blends. As part of the tested mechanical properties of the new polymer blends, we noted the desired increase in the tensile strength, in the relative elongation at break and in the impact strength with a decrease in hardness, in particular with the presence of 5 wt.% PU. Therefore, for further improvement, hybrid nanobiocomposites with 5 wt.% PU and organically modified montmorillonite (MMT – Cloisite 30®B) were produced. The nanoadditive was used in typical amount of 1-3 wt.%. The nanostructure of the biocomposites produced by extrusion was examined by small-angle X-ray scattering (SAXS) and transmission electron microscopy (TEM), the morphology by scanning electron microscopy (SEM), and compatibility by infrared spectroscopy (FT IR). In addition, selected mechanical properties were determined and thermal properties were tested by the thermogravimetric analysis (TGA) and the standard differential scanning calorimetry (DSC). The polyester and polyurethane chains penetrated into the interlayer spaces of organically modified nanoclay – Cloisite®30B and the complete delamination occurred during direct mixing in the extrusion process. FT IR spectral analysis showed the compatibility of the polymer biocomposite components by the coexistence of intermolecular interactions in the form of hydrogen bonds. The morphology studies of the produced hybrid nanobiocomposites showed an interaction of the biopolymer matrix with PU and Cloisite®30B and the formation of easily migrating polyester-polyurethane-montmorillonite adducts, which resulted in improved mechanical properties compared to the properties of the native P3HB and P3HB-PU compositions. The influence of the presence of a nanofiller on the properties of the prepared nanobiocomposites was tested and it was found that, as expected, the smallest amount of nanofiller provides the best results.It was found that the obtained nanobiocomposites containing the smallest amount of nanofillers, i.e. 1 wt.% Cloisite®30B exhibited the best mechanical and thermal properties. The desired decrease in hardness by 15% and a higher value of impact strength by 15%, an

 doi:10.20944/preprints202310.2030.v1

increase in elongation at break by 60% and an increase in thermal stability of the newly produced biocomposites compared to to the native P3HB were observed. The prepared nanobiocomposites combined the best features caused by the elasticizing effect of polyurethane and the formation of P3HB-PU-MMT adducts.

Keywords: polyhydroxyalkanoates; poly(3-hydroxybutyrate); composites; nanocomposites; structure-properties relationship

1. Introduction

Plastics are used in almost every field, from the automotive industry to medicine. With the growing awareness of environmental protection in society, biopolymers are increasingly attracting attention. These materials are replacing the previously widely used non-biodegradable polymers. Most research is based on already existing biomaterials such as polyhydroxyalkanoates (PHAs) [1,2]. These polymers can be converted into water and carbon dioxide in the presence of oxygen, and into methane in the case of anaerobic conditions.

PHAs, i.e., linear biopolyesters composed of hydroxyalkanoate units, are biodegradable and biocompatible as well as can successfully replace petroleum-based materials. The most popular polymer in the PHAs family is poly(3-hydroxybutyrate), P3HB (Figure 1) [3], known as a double green polymer, which is used in the agricultural, packaging and medical industries [4–7].

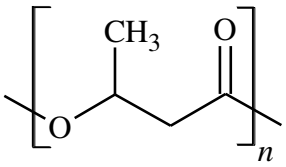

Figure 1. Repeated unit of P3HB.

Compared to other biodegradable polyesters, P3HB is a semicrystalline material with a high melting point (Tm = 173-180°C) and its glass transition temperature (Tg) is about 0-10°C Poly(3-hydroxybutyrate) is produced as an energy carrier by various bacteria [8–11], which build polymer chains that are perfectly linear and isotactic [12], allowing unique properties and a high degree of crystallinity [13]. In this form, P3HB is biobased, biodegradable and biocompatible [14–16]. The polymer is UV-resistant, and is insoluble in water and relatively resistant to hydrolysis, which distinguishes it from other biodegradable polymers that are either water-soluble or moisture-sensitive.

Therefore P3HB is a very interesting material, a substitute for synthetic polypropylene. P3HB can be extruded, injected and pressed using conventional processing equipment. Unfortunately, storage of P3HB products at room temperature causes deterioration of product properties, and the material becomes very brittle due to the formation of significant proportions of the crystalline phase [17]. Such disadvantages of P3HB, *i.e.* increased stiffness and brittleness, and above all, low thermal stability, only slightly higher than its melting point [18], limit the large-scale commercial use of P3HB. The thermal instability of this polymer during plasticization renders the replacement of commercial non-biodegradable polymers with native P3HB difficult due to the narrow window of processing conditions.

In order to improve the properties of P3HB and increase its range of applications, the polymer must undergo multiple modifications [19]. The manufacture of polymer blends and composites based on the P3HB matrix leads in most cases to the desired separation of its melting point and degradation temperature, which is characterized by better thermal properties and at the same time better mechanical properties.

Preprints (www.preprints.org) | NOT PEER-REVIEWED | Posted: 31 October 2023 doi:10.20944/preprints202310.2030.v1

The use of a polyurethane modifier will not only allow the desired modification of the thermal and mechanical properties of P3HB and its copolymers, but also accelerate its biodegradation, as the addition of hydrophilic polymers increases the absorption of water into the polymer mass and accelerates its hydrolysis [20]. In addition, polymer compositions with thermoplastic characteristics produced based on P3HB will still be highly biocompatible like native P3HB

In order to improve the properties of P3HB, especially thermal and mechanical ones, polymer compositions and composites based on it were produced. The study deals with the preparation of polymer compositions involving poly(3-hydroxybutyrate) and aliphatic linear polyurethane obtained by reacting hexamethylene 1,6-diisocyanate (HDI) with 1,4-butanediol and hybrid nanobiocomposites based on P3HB matrix with the above-mentioned polyurethane modifier with organically modified montmorillonite (Cloisite®30B) as well as study of the morphology, nanostructure, thermal and mechanical properties of the obtained materials.

2. Materials and Methods

2.1. Materials

P3HB was supplied by Biomer (Krailling, Germany); its weight average molecular mass was M_w = 443,900 g·mol^{-1} and its dispersity index was ($M_w \cdot M_n^{-1}$) = 5.72; the P3HB melt flow index was 0.11 g·(10 min)$^{-1}$ (180°C at 2.16 kg). Organically modified montmorillonite - Cloisite®30B was supplied by Southern Clay Products Inc. (Gonzales, LA, USA). Cloisite®30B is a natural montmorillonite modified with methylbis(2-hydroxyethyl) tallowalkylammonium cations. Hexamethylene 1,6-diisocyanate (HDI) and dibutyltin dilaurate (DBTL) were purchased from Sigma-Aldrich (Saint Louis, MO, USA), and 1,4-butanediol, 98%, from Aldrich (Germany) and acetone from Chemsolute (Germany).

2.1.1. Synthesis of linear polyurethane

First, 1,4-Butanediol, dried acetone and dibutyltin dilaurate were introduced into a three-necked round-bottom flask equipped with a mechanical stirrer, thermometer and dropper. Then, an appropriate amount of hexamethylene 1,6-diisocyanate (HDI) was dropped into the mixture with a molar ratio of isocyanate groups to hydroxyl groups of the diol to be 1 : 1.08. The rate of dropping was adjusted to keep the temperature of the reaction mixture below 25°C. The synthesis was monitored on the basis of isocyanate number determination according to the standard (PN-EN 1242, 2006). During the reaction (Figure 2), a product precipitated out of solution. The polyurethane was separated by filtration and was brought to a constant mass by exposure in a vacuum dryer at the temperature range of 40 – 100°C. The molar mass of the polyurethane was 109,000 g·mol^{-1} and the hydroxyl number 277 mg KOH·g^{-1}.

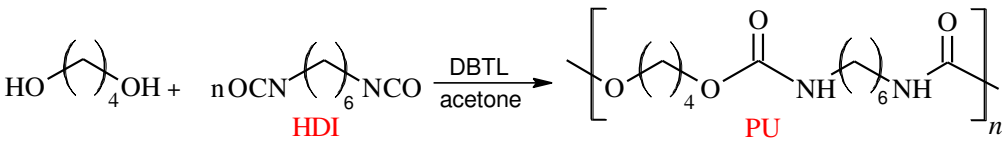

Figure 2. Synthesis scheme of polyurethane.

2.1.2. Preparation of polymer blends

In order to prepare P3HB-polymer blends with polyurethane (PU), P3HB was dosed into a Stephan-type mixer, followed by polyurethane in appropriate amounts, i.e., 5, 10, 15 and 20 wt.%. The mixture was homogenized by stirring at room temperature for about 20 minutes. Table 1 shows the composition of the resulting mixtures. The homogeneous mixture was then dosed into a hopper of co-rotating twin-screw extruder with a screw operating diameter of D = 25 mm and L/D = 33, operating at a speed of 300 – 450 rpm. The different zones of the extruder were maintained during

Preprints (www.preprints.org) | NOT PEER-REVIEWED | Posted: 31 October 2023 doi:10.20944/preprints202310.2030.v1

extrusion at the following temperatures: hopper – 31 – 32°C, II zone – 124 – 134°C, III zone – 142 – 167°C, IV zone – 135 – 136°C, V zone – 135 – 136°C, VI zone – 148 – 149°C, VII zone – 148°C, VIII zone – 148-150°C, IX zone – 148 – 151°C, and head at temperature range between 172°C and 179°C. During extrusion, volatile particles were discharged by atmospheric degassing, and the temperature of extruder head and the heating zones of extruder plasticizing system were kept constant. The melted composition was cooled in a cooling bath, pelletized and dried at 60°C for 2 hours.

2.1.3. Preparation of polymer nanobiocompositions

Polymer nanobiocomposites based on P3HB matrix with P3HB, 5 wt.% PU and 1, 2 and 3 wt.% organic nanoclay Cloisite®30B were prepared using a mixer, in which P3HB, PU and Cloisite®30B were mixed according to the composition given in Table 1. The mixing process lasted for about 20 minutes. The homogenized mixture was extruded using a co-rotating twin-screw extruder, under conditions similar to those described above in p. 2.1.2.

Table 1. Composition of the polymer mixtures.

Content [wt.%]			Sample designation
P3HB	**PU**	**Cloisite®**	
95	5	0	K5
90	10	0	K10
85	15	0	K15
80	20	0	K20
94	5	1	K5-1
93	5	2	K5-2
92	5	3	K5-3

2.2. Analytical methods

The isocyanate group contents were determined according to the standard (PN-EN 1242, 2006). The hydroxyl number was determined according to the standard (PN-92/C-8905203, 1985).

2.2.1. Small Angle X-Ray Scattering

Small Angle X-Ray Scattering (SAXS) technique was used to characterize the nanoclay structure in the prepared nanobiocomposites. The measurements were conducted at laboratory temperature using a Bruker SAXS Nanostar-U X-ray diffractometer. The spectra of samples were studied in transmission mode. The small-angle diffractometer is connected to a CuKa-filtered radiation source (1.54 Å) placed in a sealed tube, operating at 50 kV and 30 mA. A 2D detector (Vantec2000) was used to scan the entire surface of the sample, a spot beam of about 500 micrometers. The scanning range was determined by varying the distance of sample from the detector. The detector's resolution and angular range allowed measurements of 2048x2048 pixels. The measurements were conducted from 1 to 28° for a period of 2 hours.

2.2.2. Transmission electron microscopy

Transmission electron microscopy (TEM) was used to study the obtained nanostructured nanobiocomposites. The measurements were conducted on a TECNAI G12 Spirit-Twin instrument (LaB6 source) equipped with an FEI Eagle 4k CCD camera operating at an acceleration voltage of 120 kV. Prior to analysis, The samples were cut with a cryoultramicrotome and placed on 300 mesh copper grids.

 doi:10.20944/preprints202310.2030.v1

2.2.3. Scanning electron microscopy

The extruded base P3HB, P3HB-PU polymer blends and prepared nanobiocomposites were studied using a JEOL type JSM-6490 LV scanning electron microscope to analyze the morphology of materials in the micro-area. First, the process of freezing the samples in liquid nitrogen was carried out, followed by their breakage using a blade. The samples thus prepared were coated with a layer of gold about 10 nm thick using a JEOL JFC-1300 gold sputtering machine. Microphotographs showing the morphology were taken along with the surface structure of P3HB matrix blends and nanobiocomposites.

2.2.4. FTIR sectroscopy

Infrared spectra of base P3HB, PU, polymer blends and hybrid nanobiocomposites were measured using an ALPHA FT-IR spectrometer performing measurements at the wave number of 400 – 4000 cm^{-1}. The spectra were recorded at a resolution of 0.01 cm^{-1} using the ATR technique.

2.2.5. Mechanical properties

The specimens for mechanical testing were obtained by injection molding using an Arburg 420 M injection molding machine of the Allrounder 1000-250 type. The process was carried out at 140 – 172°C. The injection molding temperature was 25°C for P3HB and 30°C for polymer blends and nanobiocomposites.

The tensile mechanical properties were determined in accordance with PN-EN ISO 527-2:2012 using an "Instron 4505" testing machine. Tensile strength and relative elongation at break were measured using a rate of 5 mm/min. Unnotched Charpy impact tests were performed in accordance with PN-EN ISO 179-1:2010 using a Zwick 5102 impact hammer. Shore hardness was determined in accordance with PN-EN ISO 868 using a Zwick apparatus.

2.2.6. Thermogravimetric analysis

Thermogravimetric analysis (TGA) of P3HB and its blends as well as hybrid nanobiocomposites was carried out using a Metler Toledo TGA/DSC 3+ thermogravimetric analyzer. The heating rate of samples was 5°C·min^{-1} in the temperature range from +25 to +600°C. The measurements were conducted in a nitrogen atmosphere. The following temperatures were determined: temperature of the beginning of decomposition (T_{on}), temperature of half mass loss (50%), temperature of the maximum decomposition rate (T_{max}) and the total mass loss of sample at 600°C.

2.2.7. DSC analysis

Differential Scanning Calorimetry (DSC) measurements were conducted for P3HB, its blends and nanobiocomposities using a differential scanning calorimeter, which provided results in the form of heat flux versus temperature as a response to a linear change in temperature over time. Measurements of heat flow rate in the temperature range from -90 °C to 195 °C (from 183.15 K to 468.15 K) were carried out using a differential scanning calorimeter (DSC), a type of the Discovery DSC 2500, from TA Instruments, Inc (New Castle, DE, USA). In each case, the analyses were carried out in an atmosphere of nitrogen with a constant flow rate of about 50 ml·min^{-1}. Calibration of temperature and heat flux in the calorimeters was carried out with respect to the melting parameters of indium, i.e., the initial melting temperature, the so-called "onset," of $T_{m(onset)}$ = 156.6°C (429.6 K) and the enthalpy of fusion $H\Delta_f$ = 28.45 J·g^{-1} (3.28 kJ·mol^{-1}).

3. Results and discussion

3.1. Polymer blends of poly(3-hydroxybutyrate) – polyurethane

Polyurethane synthesized by reacting 1,4-butanediol with hexamethylene 1,6-diisocyanate was used to produce polymer blends with P3HB and 5, 10, 15 and 20 wt.% of PU (as shown in Table 1)

Preprints (www.preprints.org) | NOT PEER-REVIEWED | Posted: 31 October 2023 doi:10.20944/preprints202310.2030.v1

and improve the mechanical and thermal properties of aliphatic polyester. The polymer blends were prepared by melting homogenization using a co-rotating twin-screw extruder. A base P3HB was also processed to obtain a reference material under comparable conditions.

3.2. Spectral analysis of the produced polymer compositions

Fourier-transform infrared spectroscopy (FTIR) was used to study the interactions between P3HB and PU. Figure 3 shows FTIR spectra of P3HB, PU and their blends. The FTIR spectrum of P3HB illustrates the characteristic valence vibration band of carbonyl group in the ester structure at 1718 cm^{-1} and the vibration bands of asymmetric and symmetric C-O bonds in the ester at 1271 and 1129 cm^{-1}. Bands above 3000 cm^{-1} are not present.

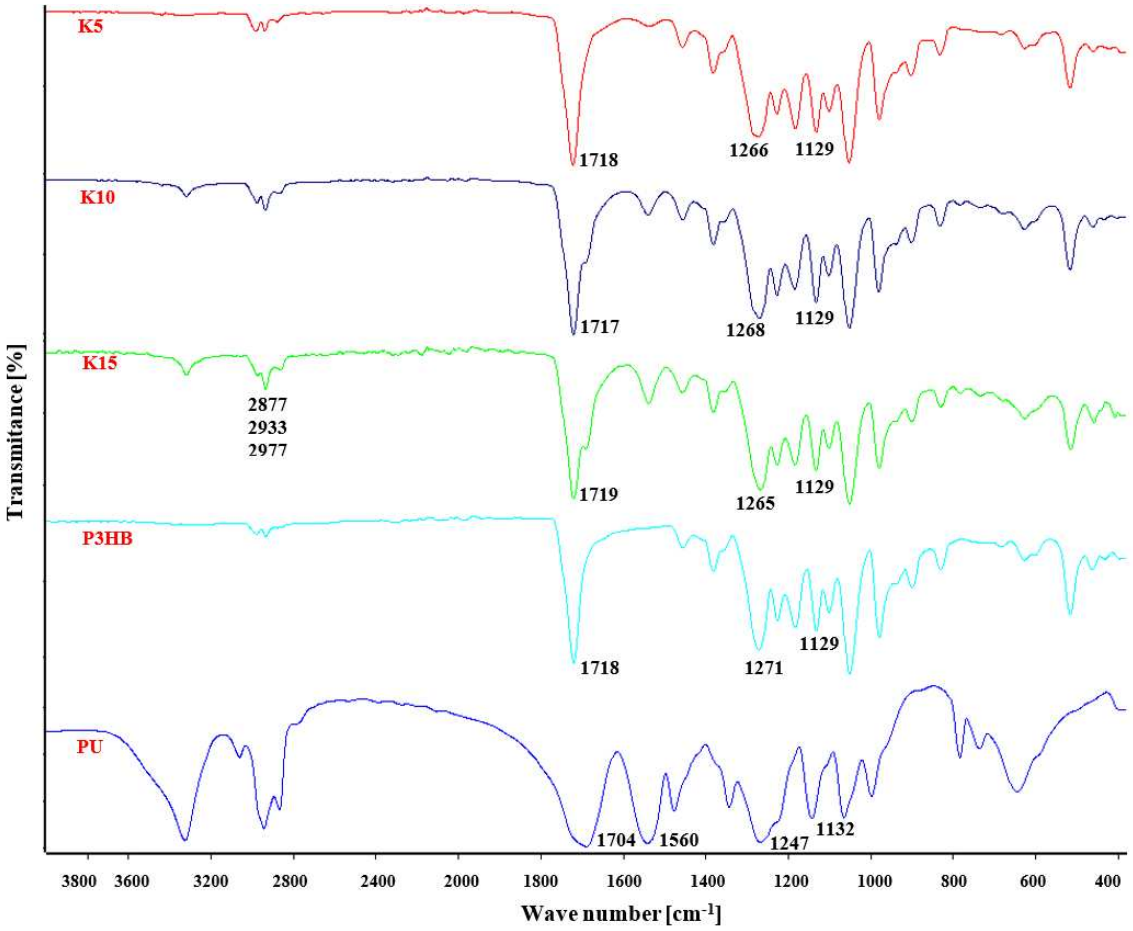

Figure 3. FTIR spectra of P3HB, PU and their blends containing 5, 10 and 15 wt.% PU.

On the other hand, the FTIR spectrum of polyurethane (Figure 3) shows the valence vibration bands of N-H bonds of the urethane group above 3100 cm^{-1}. The valence vibrations of the carbonyl group in the urethane group generate a band at 1704 cm^{-1}, while the vibrations of the CO-NH bonds are visible at 1560 cm^{-1}. Bands resulting from symmetric and asymmetric vibrations of the C-O bond in the urethane group are visible at 1247 and 1132 cm^{-1} (Figure 3).

In the FTIR spectra of P3HB-PU blends for wavenumbers above 3000 cm^{-1} there was a change in the shape of band compared to the spectrum of PU. Its' intensity decreased significantly and it is broadened, which is due to the formation of hydrogen interactions involving the urethane groups and/or terminal hydroxyl groups of aliphatic polyurethane, with the ester groups of P3HB (Figure 4) [21,22].

Preprints (www.preprints.org) | NOT PEER-REVIEWED | Posted: 31 October 2023 doi:10.20944/preprints202310.2030.v1

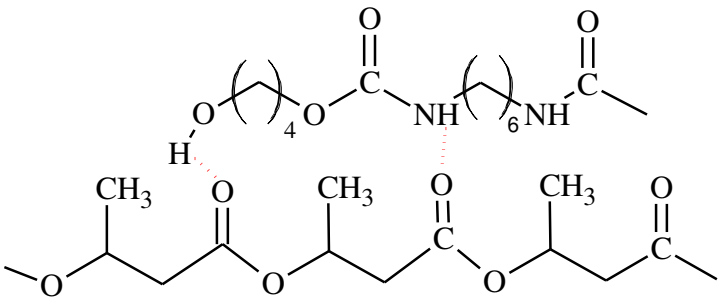

Figure 4. Scheme of hydrogen bond formation between P3HB od PU chains.

The intensity of the band above 3000 cm^{-1} increases with the PU content in the polymer mixture (Figure 3). In the range of 2800 – 3000 cm^{-1}, there are 3 bands of asymmetric and symmetric C-H bonds of methyl and methylene groups at 2877, 2933 and 2977 cm^{-1}, similar to the spectrum of P3HB or PU. Only one broadened valence vibration band of carbonyl groups in ester and urethane groups is observed at 1719 cm^{-1}. Asymmetric and symmetric C-O bond vibration bands occur together for ester and urethane groups at 1268 cm^{-1} and 1129 cm^{-1}.

3.3. Morphology analysis of the obtained polymer compositions

Scanning electron microscope (SEM) micrographs of the fractured surfaces at the point of load application were taken to investigate the changes in the morphology of prepared polymer mixtures compared to polymer P3HB matrix. The surface of base P3HB, shown in Figure 5, has a slightly wavy, glassy morphology, which along with several edge lines, indicates the presence of a regular crack propagation path. Such morphology suggests a relatively brittle behavior.

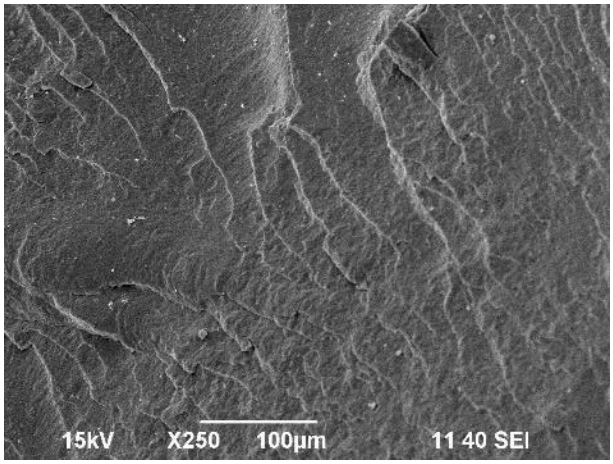

Figure 5. SEM micrograph of base P3HB.

Figure 6 shows SEM micrographs of the samples fracture surfaces of poly(3-hydroxybutyrate) blends with 5, 10, 15 and 20 wt.% of a polyurethane modifier. The images of fractured samples allow to explain the mechanism of improvement of the mechanical properties of the nanobiocomposites tested by the added polymeric modifier. The presented images were obtained by scanning the fracture surfaces of tested samples at the site of their cracking as a result of the applied load. The fracture surfaces of all P3HB/PU blends shown in Figure 6 are slightly wavy and glassy, indicating the presence of a regular and reltively linear crack propagation path, which is typical of brittle materials. As can be noted, the introduction of PU as a modifier caused an apparent disruption of the continuity of P3HB matrix structure. One can also note the appearance of crystalline domains in the form of rough platelets arranged unidirectionally. This may suggest the interaction of biopolymer matrix with polymeric modifier (PU) resulting in disentanglement of interacting P3HB chains and formation of the mentioned domains [23].

Preprints (www.preprints.org) | NOT PEER-REVIEWED | Posted: 31 October 2023 doi:10.20944/preprints202310.2030.v1

However, it can be noted that disentanglements increased with increasing amount of PU in the P3HB matrix. These disentanglements may be related to an increase in elongation, impact strength of the tested blends as the polymer modifier content increased, and enhancement of the mentioned mechanical properties are due to the flexibilization of the polyester matrix by the PU modifier. If the phase separation is not detectable, the blends give optimum mechanical and thermal properties results. Urethanes groups of PU and terminal hydroxyl groups are able to intereact with of P3HB ester groups forming hydrogen bonds. The good ductile properties are achieved by the strong interactions exerting between P3HB and PU chains [22,24].

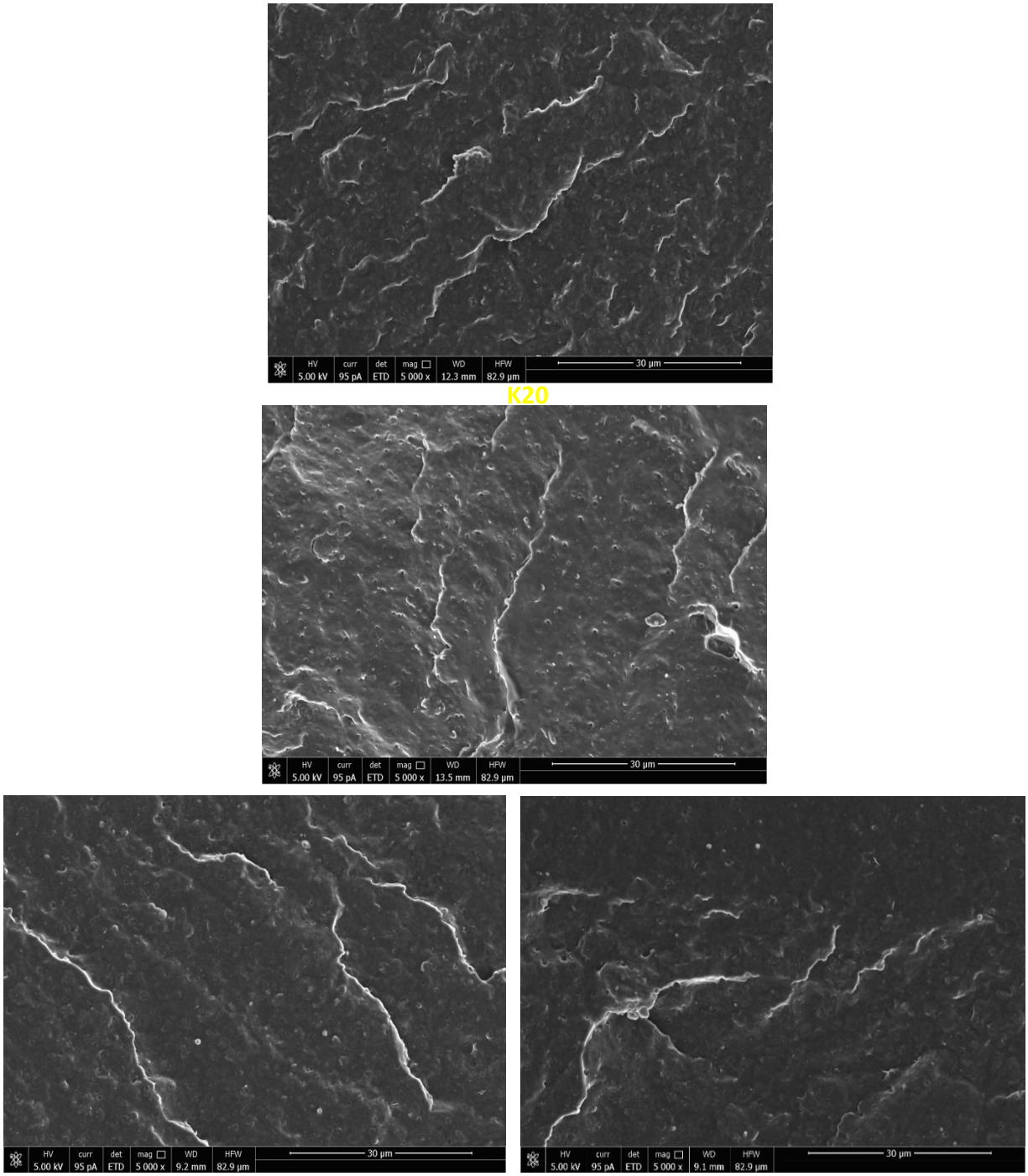

Figure 6. SEM micrographs of P3HB polymer compositions with 5, 10, 15 and 20 wt.% PU, designated K5, K10, K15 and K20, respectively.

Preprints (www.preprints.org) | NOT PEER-REVIEWED | Posted: 31 October 2023 doi:10.20944/preprints202310.2030.v1

3.4. Mechanical properties of the prepared P3HB-PU polymer blends

Selected mechanical properties of the obtained polymer blends were investigated by measuring, among others, the tensile strength and the relative elongation at break. Figure 7a shows the obtained strength results as a function of the amount of added polyurethane modifier. The tensile strength of P3HB-PU polymer blends depends on the modifier (PU) content, and it increased to a maximum value at 5 wt.% PU in the blend, then decreased with increasing PU content. Some authors have reported a trend of decreasing tensile strength in several plasticized polymers with increasing plasticizer content with a slight increase in elongation at break [25–27]. This finding might be explained by the increase of free volume in the system due to flexible chains of modifier addition, leading to reduction of specific polymer/polymer interactions.

The values of relative elongation at break shown in Figure 7b have a similar tendency, i.e., they maximally increased after the addition of 5 wt.% PU, and then decreased up to a content of 15 wt.% PU. Further increase in the proportion of PU in the blend did not change the values of relative elongation at break.

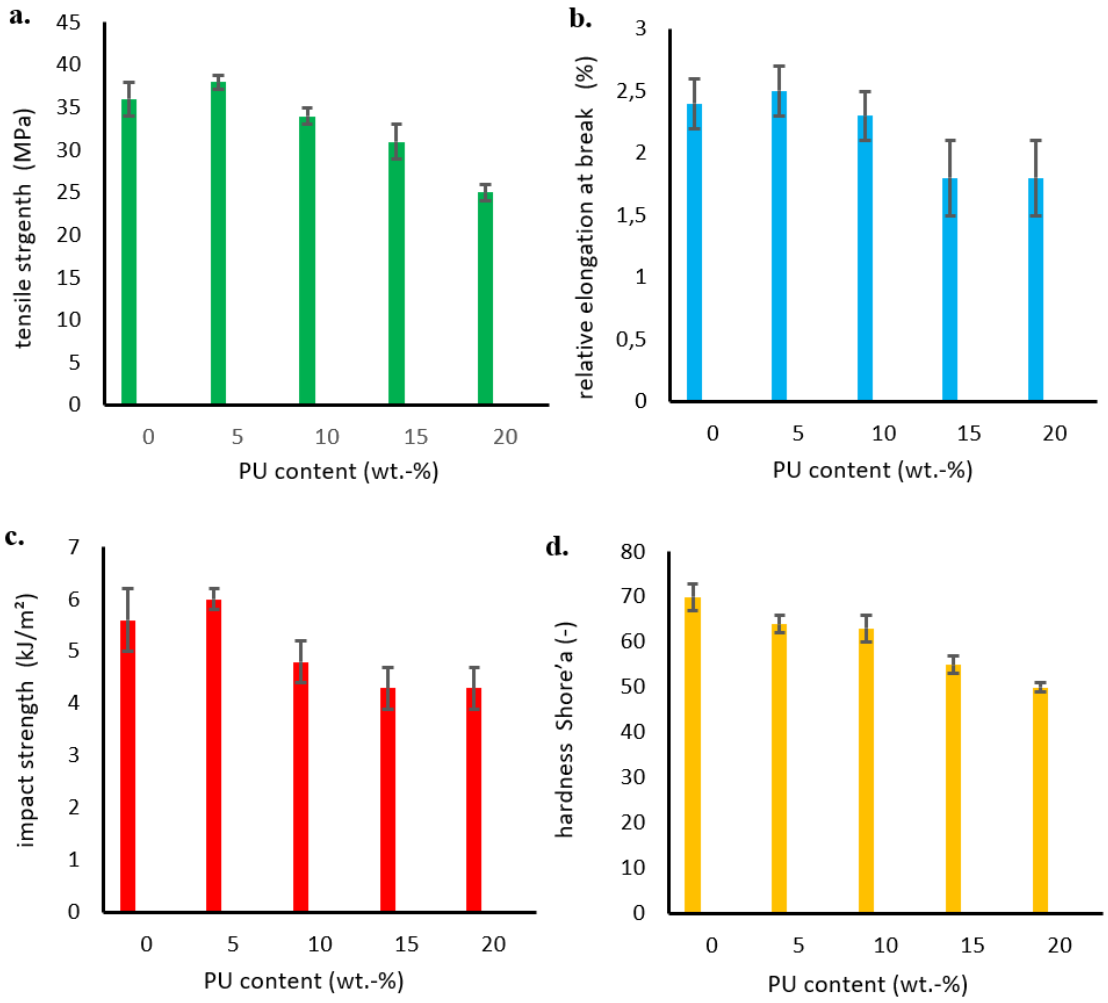

Figure 7. Tensile strength (a), relative elongation at break (b), impact strength (c), and hardness (d) of P3HB-PU polymer compositions as a function of the amount of PU introduced.

As shown in Figure 7c, the impact strength (IS) of the obtained polymer blends also increased compared to unmodified P3HB, with a maximum value at 5 wt.% PU. However, a further increase in the PU content resulted in a decrease of the impact strength below that of base P3HB. The introduction of more than 15 wt.% PU no longer changed the impact resistance of the resistance of the blends. Similar findings were reported by Seydibeyoglu *et al.* [26] and by Jostet al. [28]. The maximum iimprovement of all measured mechanical properties with a addition of small amount of

 doi:10.20944/preprints202310.2030.v1

polymeric modifier (i.e. 5 wt.% PU) can be attributed to the formation of grafted interpenetrating polymer network structure as reported elsewhere with similar crosslinkable systems. Moreover, the hardness of prepared P3HB was found to decrease with increasing modifier content (Figure 7d). The decrease in hardness may be due to the softening effect and flexibilization of the samples induced by the consequent increase in free volume in the mixture and the presence of flexible modifier chains [29].

3.5. Thermal stability of the produced P3HB polymer blends

The thermal stability of P3HB polymer blends with 5, 10, 15 and 20 wt.% PU content was investigated by thermogravimetric analysis (TGA). The results of TGA are shown in Table 2. The introduction of polyurethane into P3HB caused an increase in the degradation temperature of the resulting polymer mixture compared to unmodified P3HB. The polymer sample containing 5 wt.% PU started to degrade at 234°C, which is 22°C higher than the P3HB without modifier. Adding more polyurethane made the thermal stability even higher. The onset of decomposition temperatures are 266, 268 and 268°C for K10 and K15 and K20, respectively. The thermal degradation of the P3HB-PU polymer samples, just as unmodified P3HB, proceeded in one single step with the presence of a peak on the DTG curve representing the fastest decomposition at 278-280°C. The mass of the residue at 600°C did not exceed 1 wt.% (Table 2). The addition plasticizer led to a noticeable improvement in the thermal stability of P3HB, which is achieved by the interaction of the plastisizer molecules and the polyester chain. It resulted in the formation of a thin physical barrier on the surface of the blends and obstructed permeability of volatile products towards the exterior. It effectively retarded the thermal degradation of blends as explained in other studies [30–34].

Table 2. Interpretation of TG and DTG curves of P3HB-PU polymer compositions and hybride nanobiocomposites recorded at heating rate of 5°C/min in the nitrogen atmosphere.

Sample	T_{on} [°C]	$T_{50\%}$ [°C]	T_{max1} [°C]	Residue 600°C [wt.%]
P3HB	212	246	278	1.01
K5	234	268	278	0.94
K10	266	277	278	0.75
K15	268	279	280	0.86
K20	268	279	279	0.64
K5-1	245	279	279	1.58
K5-2	245	279	278	2.64
K5-3	241	278	276	3.65

3.6. Thermal properties of P3HB - PU polymer blends

In order to analyze the thermal properties of prepared blends of P3HB and polyurethane, DSC measurements were conducted. Figure 8 shows the dependence of the experimental heat flow of tested blends as a function of temperature at a heating rate of 10°C·min^{-1} in the temperature range of -90°C to 195°C after prior cooling at the same rate in the temperature range given.

Preprints (www.preprints.org) | NOT PEER-REVIEWED | Posted: 31 October 2023 doi:10.20944/preprints202310.2030.v1

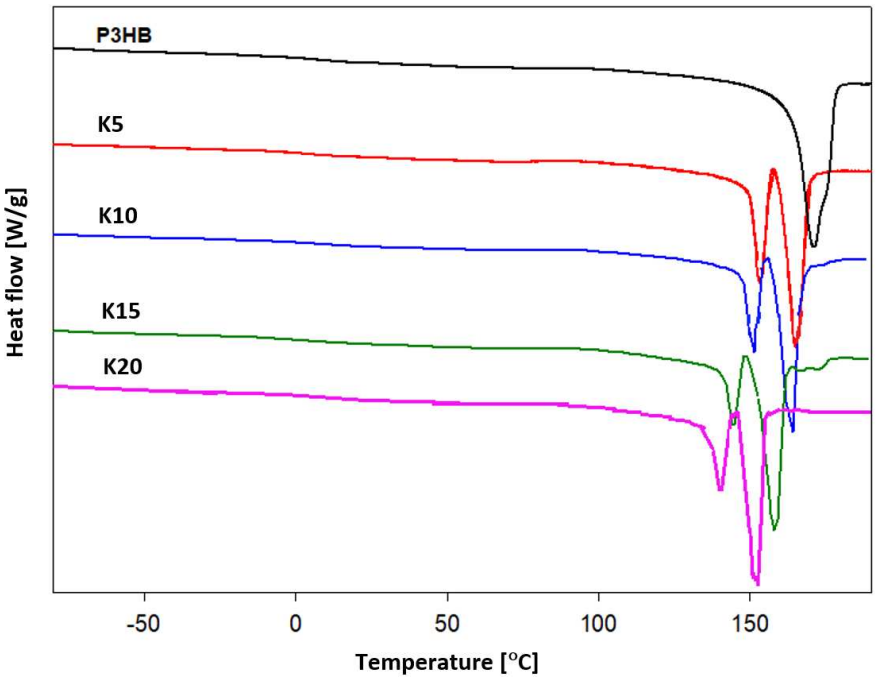

Figure 8. Comparison of heat flows of P3HB and its polymer compositions with PU as a function of temperature upon heating at a rate of 10°C·min^{-1}.

Qualitative thermal analysis was performed on the basis of heat flow rates of semicrystalline P3HB and its blends with polyurethane and recording only glass transition (T_g) and melting processes. Based on the analysis of glass transition region during heating, the change of specific heat (ΔCp) and the value of glass transition temperature T_g were determined. In turn, from the analysis of melting region, the heat of fusion ΔH_f and the melting temperature $T_{m(peak)}$ were estimated. The occurrence of two peaks in the melting of polymers may indicate the coexistence of different crystalline forms or may be due to the introduction of PU. Two melting peaks were observed in thermograms of all polymer samples. The first, always smaller endothermic peak is due to the melting of less stable crystals ($T_{m1\ (peak)}$, Table 3), while the second larger peak ($T_{m2\ (peak)}$, Table 3) corresponds to the melting of larger, more formed crystals. It should be noted that the melting onset temperature $T_{m\ (onset)}$ of the polymer samples was lower than that of unmodified P3HB and decreased regularly with increasing polyurethane content in the mixture [29]. A decrease in the glass transition temperature of the new polymer mixtures was also observed, which proves the plasticization of the polyester due to the introduction of polyurethane. Similar effect was observed by Fernández-Ronco et al [35] in P3HB - poly(butylene succinate-butylene dilinoleate) blends or by Kozlowska et al. [36].

Table 3. Comparison of thermal parameters of P3HB-PU polymer blends upon heating their representative samples at 10°C·min^{-1} after prior cooling at the same rate.

Sample	T_g [°C]	ΔC_p [J·g^{-1}·°C^{-1}]	$T_{m\ (onset)}$ [°C]	T_{m1} [°C]	T_{m2} [°C]	ΔH_f [J·g^{-1}]	T_c [°C]	ΔH_c [J·g^{-1}]
P3HB	7.70	0.1620	159.73	165.75	-	91.93	90.50	88.79
K5	4.45	0.2257	149.92	153.30	165.30	92.98	88.00	79.06
K10	6.02	0.0680	145.03	150.95	163.50	88.14	85.60	68.98
K15	2.40	0.2294	140.81	144.55	158.10	94.55	80.80	67.04
K20	2.30	0.1875	135.53	140.12	153.20	92.67	76.40	66.00

The estimated thermal parameters of the phase transitions are presented in Table 3. The heat of crystallization ΔHc and the crystallization temperature Tc were determined during the cooling analysis. The presence of polyurethane caused a decrease in the crystallization temperature, which regularly decreased with an increase in the amount of PU introduced (Table 3).

Preprints (www.preprints.org) | NOT PEER-REVIEWED | Posted: 31 October 2023 doi:10.20944/preprints202310.2030.v1

3.7. Production of hybrid nanobiocomposites

Taking into account the obtained results of P3HB-PU polymer blends and with a view for further improvement of the physical properties of P3HB, hybrid nanobiocomposites were obtained by using polyester as a matrix, with the addition of the above-mentioned aliphatic linear polyurethane as a modifier and organic-modified montmorillonite – Cloisite®30B as a nanofiller. Polyurethane at 5 wt.% and Cloisite®30B at 1, 2 and 3wt.% were used to produce the nanocomposites.

3.8. FT IR analysis of hybrid nanobiocomposites

FT IR spectra of hybrid nanobiocomposites based on P3HB matrix with PU and Cloisite®30B as modiers are shown in Figure 9. A small band above 3000 cm^{-1} appears in the FT IR spectrum of the hybrid nanobiocomposites, whose intensity increased with increasing organic nanoclay content. This confirms the formation of hydrogen bonds between the urethane groups of modifier and the ester groups of polyester and modified montmorillonite [37,38]. Three bands of vibration of the asymmetric and symmetric C-H bonds of the methyl and methylene groups at 2877, 2933 and 2977 cm-1 and whose intensity increased with the increase in the amount of the nanofiller were observed in the range 2800 – 3000 cm -1. One common valence vibration band of ester and urethane C=O groups was observed at 1707 cm^{-1} and at a lower frequency than in the case of base P3HB matrix or the P3HB-PU blend (cf. Figure 1 and Figure 6), confirming the formation of intermolecular hydrogen bonds with Cloisite®30B. A common band for esters and urethanes for the vibration of asymmetric C-O bonds appeared at a wavenumber of 1270 cm^{-1}, and a band for the vibration of symmetric C-O bonds appeared at 1097 cm^{-1}, similar to the spectrum of P3HB-PU polymer blends. The spectral analysis confirms the interaction and compatibility of the components of produced hybrid nanobiocomposites.

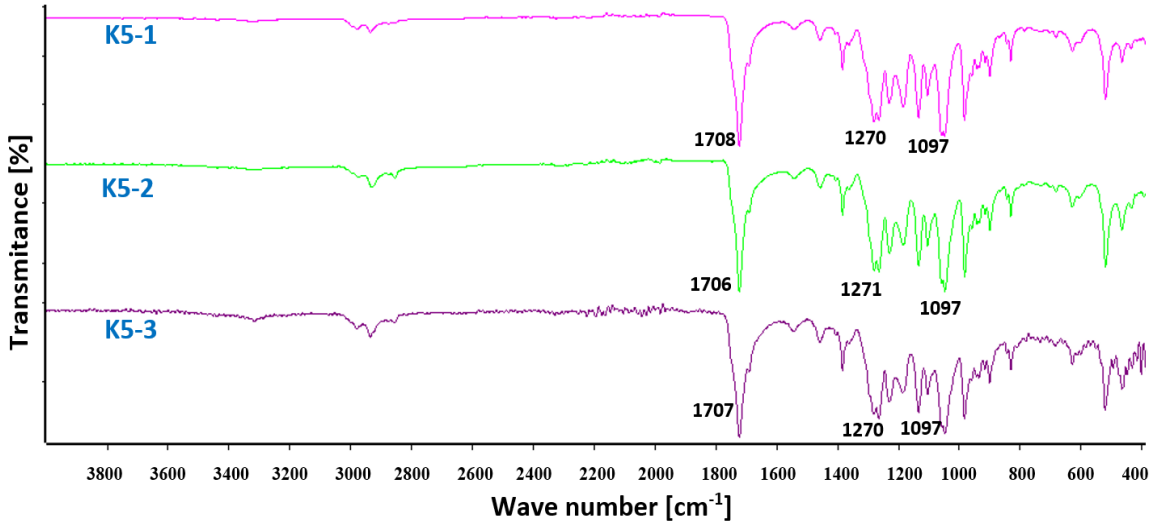

Figure 9. FT IR spectra of hybrid nanobiocomposites containing 5 wt. %. PU and 1, 2, or 3 wt. % Cloisite®30B (K5-1, K5-2, and K5-3).

3.9. Structure analysis of hybrid P3HB-PU-Cloisite®30B nanobiocomposites

In order to characterize the nanoclay structure in the obtained biocomposites, SAXS measurements were conducted in the range from 1° to 28°, with the most diagnostic area being the range 1-5°. Figure 10 shows the SAXS patterns of prepared nanobiocomposites as well as the patterns of unmodified P3HB and that of Cloisite®30B nanoclay. Unmodified P3HB shows only background scattering at an angle 2Θ of less than 12° [39,40]. In contrast, the pattern of Cloisite®30B shows a peak with a maximum with an angle 2θ of about 5.00° [41], which means a distance between the

Preprints (www.preprints.org) | NOT PEER-REVIEWED | Posted: 31 October 2023 doi:10.20944/preprints202310.2030.v1

aluminosilicate plates in Cloisite®30B of approximately 1.77 nm. The tested hybrid nanobiocomposites with 1 wt.% organic nanoclay (sample designated K5-1) and higher amount do not show a peak with a maximum angle value 2θ less than 5°. The absence of a peak in this area proves the complete delamination of Cloisite®30B, which means that the polyester and polyurethane chains not only filled the interlayer spaces of the aluminosilicate stacks, but led to their complete delamination [42]. Analysis of SAXS patterns of the produced hybrid nanobiocomposites indicates that the exfoliated structure of nanocomposites was obtained, guaranteeing a definite improvement in the properties of new materials over those of the initial matrix.

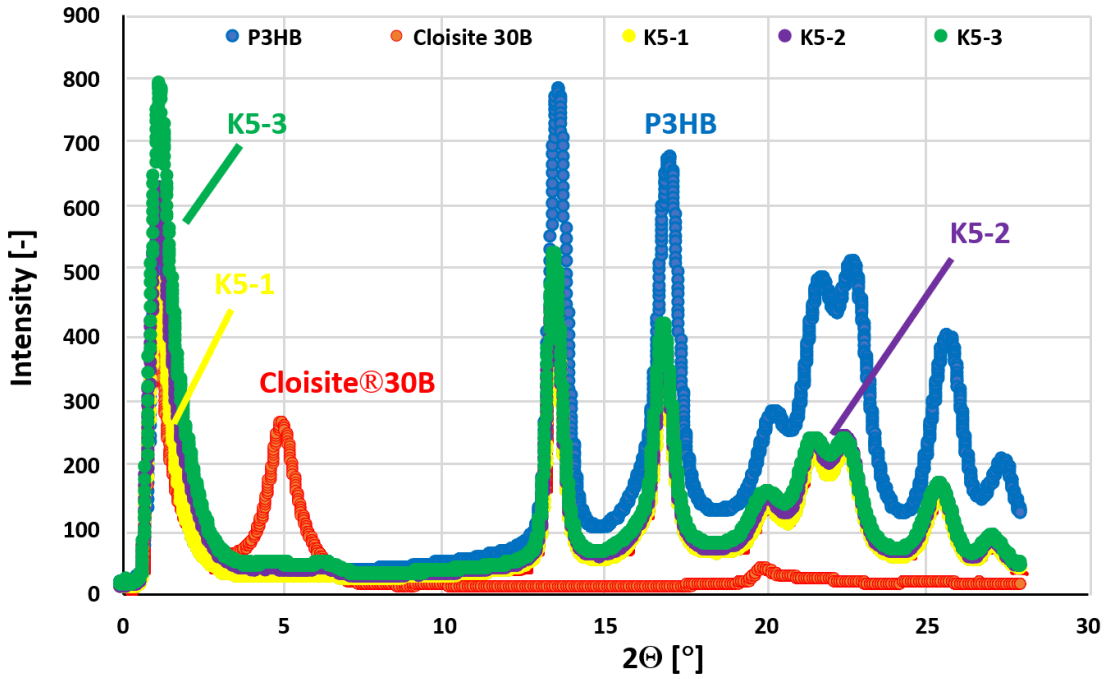

Figure 10. SAXS plots of native P3HB, Cloisite®30B - organic nanoclay and produced hybrid biocomposites, designated as K5-1, K5-2, K5-3.

3.10. Nanostructure analysis of produced hybrid nanobiocomposites

The nanocomposites were studied by transmission electron microscope (TEM) method to observe the effect of nanoclay content on nanostructure features. Selected TEM micrographs of the nanobiocomposites are presented in Figure 11. The dark lines represent cross sections of the nanoclay layers, and the gray area corresponds to the polymer matrix. Figure 11 a shows the base polyester matrix, and Figure 11 b-d shows the structure of hybrid nanobiocomposites containing 1-3 wt.% Cloisite®30B.

Preprints (www.preprints.org) | NOT PEER-REVIEWED | Posted: 31 October 2023 doi:10.20944/preprints202310.2030.v1

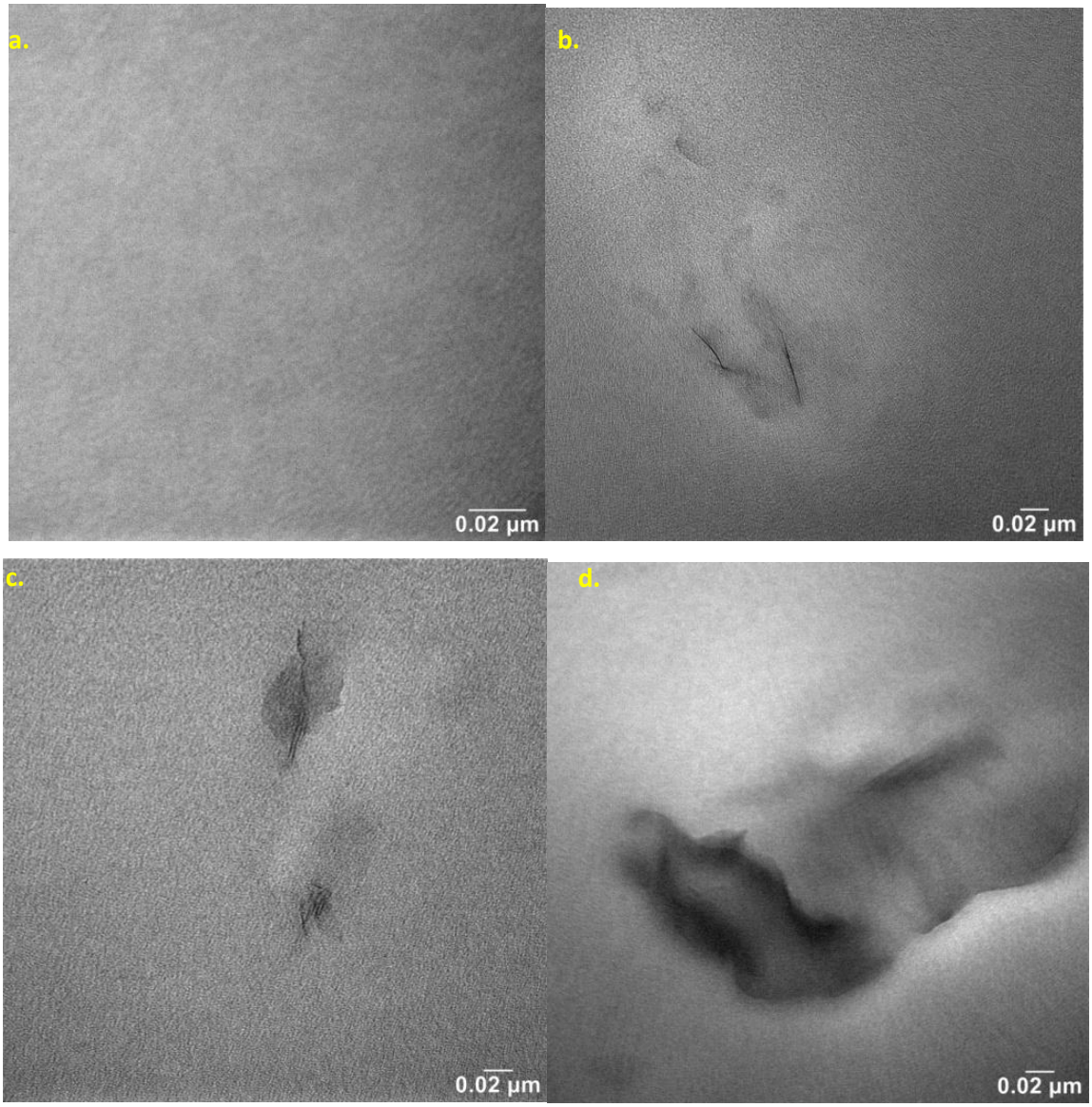

Figure 11. TEM microphotographs of P3HB-PU nanobiocomposites containing: 1, 2 and 3 wt. %. Cloisite®30, designated respectively: (a) K5-1, (b) K5-2, (c) K5-3 (the visible artifacts results from sample preparation).

Analysis of the nanocomposite structure by TEM confirmed the conclusions of SAXS analysis of the aforementioned composites. TEM micrographs (Figure 11) show that Cloisite®30B is quite susceptible to deagglomeration and dispersion in the P3HB matrix induced by the shear forces. It is important to note that single silicate nanoplates and/or small stacks of only few silicate nanoplates are not visible in TEM micrographs. As the nanofiller content decreases, the size of dispersed organic clay areas becomes smaller and smaller. The study of this image reveals a homogeneous dispersion of clay platelets throughout the matrix on a nanometer scale. The montmorillonite layers are well dispersed in the matrix in the form of randomly stratified nanosheets indicating mainly exfoliation structure [43]. Figure 11c and 11d show TEM images of hybrid nanobiocomposites with 2 and 3 wt.% Cloisite®30B, respectively. The main common observation of the micrographs presented in Figure 11 b-d is that they all show a nanoscale dispersed morphology, independent of the Cloisite®30B concentration, identified by the presence of individual clay nanosheets with no visible agglomeration. Exfoliated layers are the main structure, as evidenced by single clay nanosheets and the absence of tactoids [44].

 doi:10.20944/preprints202310.2030.v1

3.11. Morphology analysis of the obtained hybrid nanobiocomposites

Figure 12 shows Scanning electron microscope (SEM) micrographs of the fracture surfaces of poly(3-hydroxybutyrate) matrix nanocomposite samples containing 5 wt.% polyurethane (PU) modifier and different amounts of Cloisite®30B nanofiller, 1 wt.% (sample K5-1), 2 wt.% (sample K5-2) and 3 wt.% (sample K5-3), respectively. The incorporation of nanoparticles into the polyurethane flexibilized P3HB (Figure 12) resulted in a noticeable roughness in the fracture surfaces of the nanobiocomposites. Polyester matrix modified with 5 wt.% PU and the smallest amount of 1 wt.% Cloisite®30B was characterized by a noteworthy completely different morphology from that of the other samples (Figure 12 a). It is possible to observe distinct wavelike domains arranged in different directions, indicating the presence of a regular crack propagation path. These domains are larger in size and more widely spaced than in the other samples. This suggests that they are interacting less with each other and the effect of P3HB becoming more flexible [45]. This may be related to the formation of P3HB-PU-MMT adducts that are easily displaced with respect to each other, and this phenomenon may affect the significant increase in elongation and the slight increase in impact strength of the analyzed sample. On the other hand, an increase in the hardness of material may suggest a stiffening effect of MMT, which translates into the roughness of the observed nanocomposites. However, the addition of higher than 1 wt.% of Cloisite®30B (i.e. 2 wt.% or 3 wt.%), already excludes the sample K5-1 for the formation of the mentioned agglomerates. This suggests that the addition of 2 wt.% or 3 wt.%. Cloisite®30B is already pointless. The structure of samples containing 2 wt.% or 3 wt.% of Cloisite®30B (K5-2 and K5-3) (Figure 12 b and 12c) becomes similar to that of a binary polymer mixture, i.e. containing P3HB and a polymeric modifier (Figure 6). Increasing the amount of added nanoparticles above 1 wt.% does not affect the separation of the formed domains and thus the flexibility of material, which affects the decrease in impact strength, toughness and elongation at break of these nanobiocomposites and suggests the stiffening of P3HB-PU polymer blends by such amounts of Cloisite®30B (2 wt.% and 3 wt.%) [46].

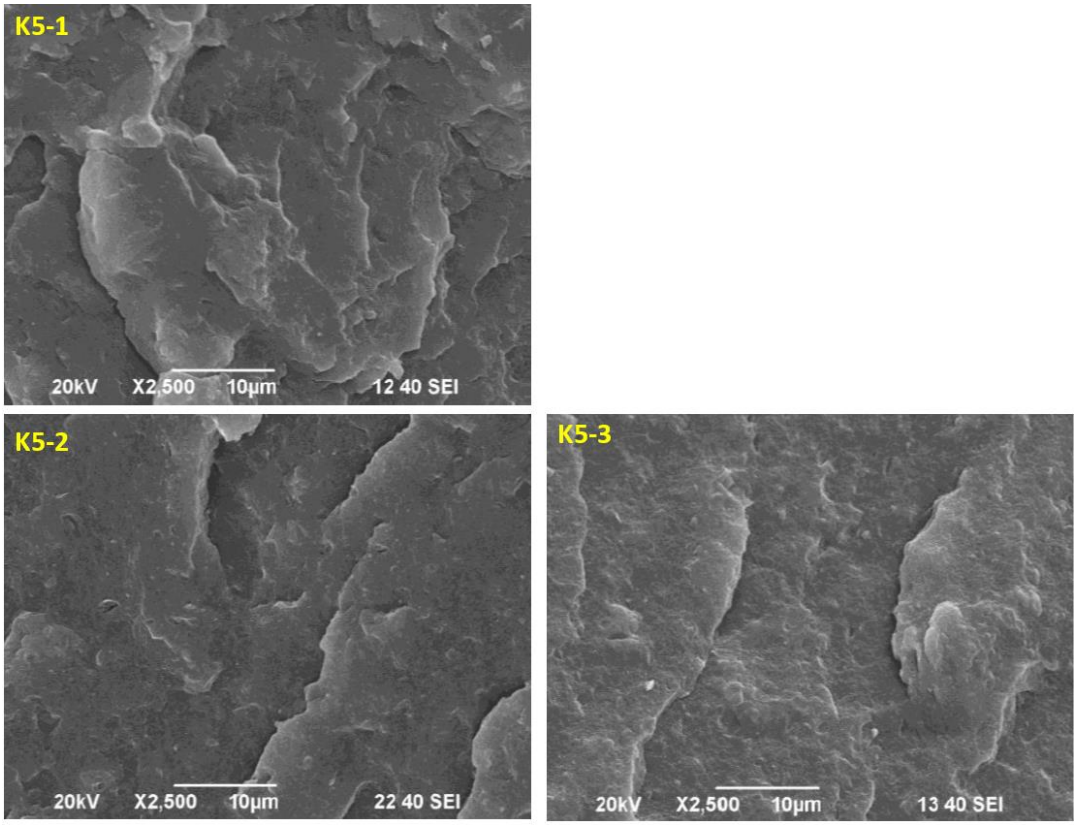

Figure 12. SEM micrographs of P3HB hybrid nanobiocomposites containing 5 wt.% PU and 1, 2 or 3 wt.% organic modified nanoclay – Cloisite®30B, designated K5-1, K5-2 and K5-3, respectively.

 doi:10.20944/preprints202310.2030.v1

3.12. Mechanical properties of the obtained nanobiocomposites hybrids

As a part of the mechanical tests, the tensile strength, relative elongation at break, impact strength and hardness of the obtained hybrid nanobiocomposites were investigated similarly to the P3HB-PU polymer blends, and the results are shown in Figure 13. The effect of nanofiller addition on the increase in tensile strength is shown in Figure 13 a. As mentioned earlier (Figure 8 a), the addition of polyurethane resulted in a slight increase in tensile strength, while the incorporation of organic nanoclay caused a noticeable increase in tensile strength (TS). Increasing the amount of nanocharge caused a decrease in TS which intensified with increasing in nanofiller content [47]. It should be noted that the tensile strength of all hybrid nanobiocomposites was higher than that of P3HB matrix. Nanoclay (Cloisite 30B) in an amount between 1 and 3 wt% had good dispersibility in the polymer matrix of PH3B-PU, which improved the mechanical properties of the biocomposites [48–50]. The simultaneous addition of 5 wt.% PU and 1 wt.% Cloisite®30B (nanobiocomposite K5-1) resulted in a large increase in relative elongation at break of about 58% compared to the P3HB matrix sample (Figure 13 b). Further increase in the percentage of modified nanoclay to 3 wt.% led to a decrease in the value of elongation at break, even below the value for unmodfied P3HB (sample K5-3).

As in the case of impact strength of the hybrid nanobiocomposites (Figure 13 c), we observe that the simultaneous addition of polyurethane and Cloisite®30B (1 wt.% of nanoclay) led to a significant increase in impact strength, by approximately 30% compared to unmodified P3HB matrix. However, the impact strength decreased for the nanobiocomposites samples designated K5-2 and K5-3, with values still higher than that of the reference sample at 3 wt.% of nanoclay [51]. The improvement in impact strength can be induced by the presence of P3HB-PU-MMT adducts identified on SEM images, while the decrease in impact strength is related to the stiffening effect due to Cloisite®30B.

A decrease in the hardness of the tested nanobiocomposites was observed (Figure 13 d). The addition of polymeric modifier made the polyester/polyurethane blend more flexible, and the greatest decrease in hardness of about 11% was observed for the sample K5 (i.e P3HB containing 5 wt.% PU). The introduction of nanofiller resulted in a relative stiffening of the plasticized structure and a slight increase in the hardness of nanocomposite slightly above the hardness value of the sample K5.

In the case of hybrid nanobiocomposites, it was noted that the lowest content of nanofiller (1 wt.%) added to 5 wt.% PU (hybrid composite (K5-1) allowed the formation of P3HB-PU-MMT adducts, exhibiting the best mechanical properties.

Preprints (www.preprints.org) | NOT PEER-REVIEWED | Posted: 31 October 2023 doi:10.20944/preprints202310.2030.v1

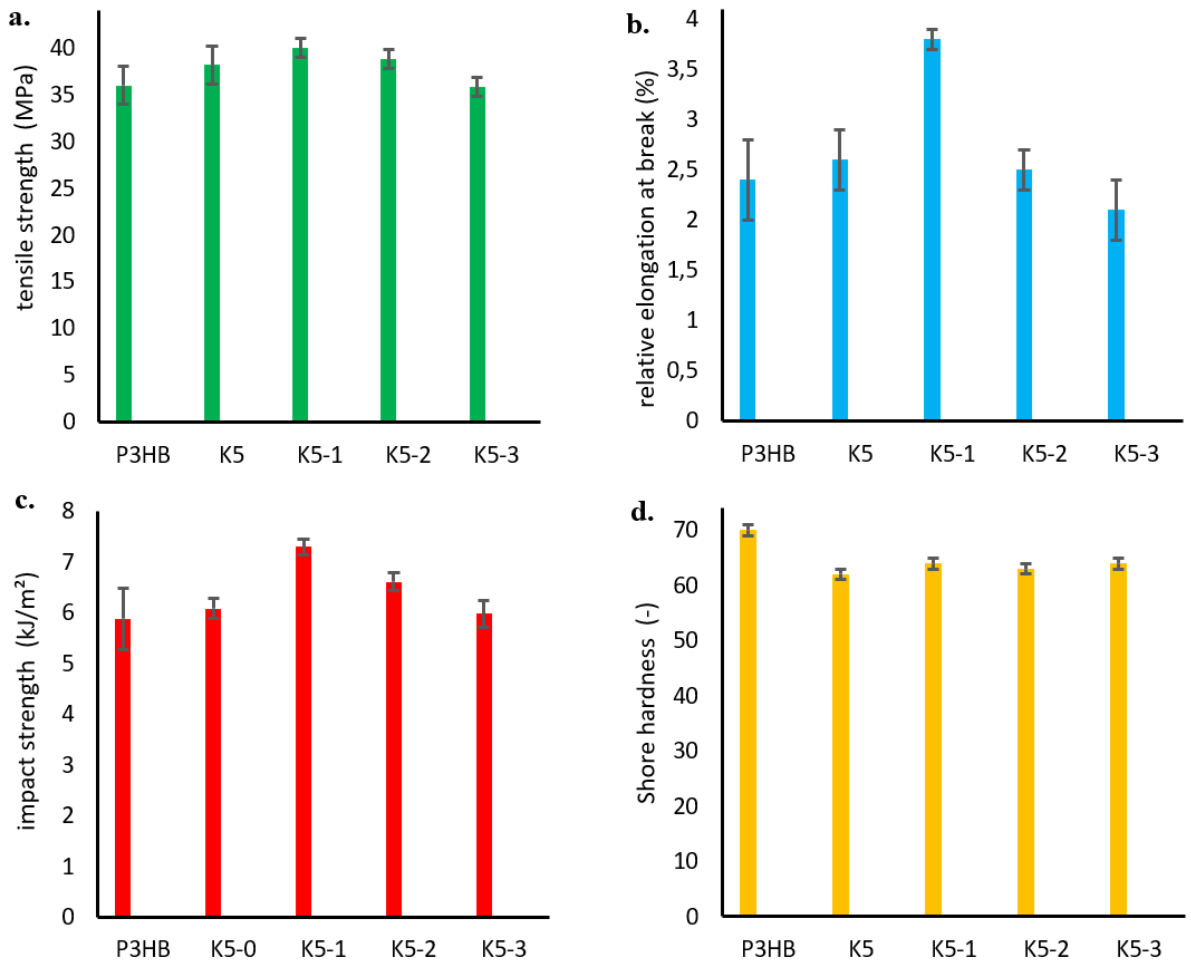

Figure 13. Dependency graph: a. tensile strength, b. relative elongation at break, c. impact strength, d. hardness of the produced hybrid nanobiocomposites as a function of Cloisite®30B content.

3.13. Thermogravimetric analysis of nanobiocomposities

The prepared hybrid nanobiocomposites were subjected to thermogravimetric analysis (TG) analysis in order to investigate the physicochemical changes that occur during heating. Thermogravimetric analysis of the nanobiocomposites (Table 2) showed that the addition of 5 wt.% aliphatic polyurethane and 1 wt.% organic nanoclay (sample K5-1) resulted in a 33°C increase in the stability of the nanobiocomposite compared to the reference P3HB sample [51–53]. With the addition of 2 wt.% nanofiller, the thermal stability remained unchanged relative to the nanocomposite containing 1 wt.% Cloisite®30B. In contrast, the addition of 3 wt.% nanoclay (sample K5-3) resulted in a slight (4°C) decrease in the thermal stability of hybrid nanobiocomposite. However, the thermal stability of this nanocomposite was still higher than that of unfilled P3HB and polyester modified with only 5 wt.% polyurethane (sample K5). Temperature of the maximum decomposition rate was similar for unmodified P3HB and its nanobiocomposites and oscillated between 279-276°C.

3.14. Thermal analysis based on the differential scanning calorimetry measurements

Figure 14 shows the heat flow rates versus temperature in the range of -90°C to 195°C for K5-1, K5-2, and K5-3 nanobiocomposites obtained based on the DSC measurements.

Preprints (www.preprints.org) | NOT PEER-REVIEWED | Posted: 31 October 2023 doi:10.20944/preprints202310.2030.v1

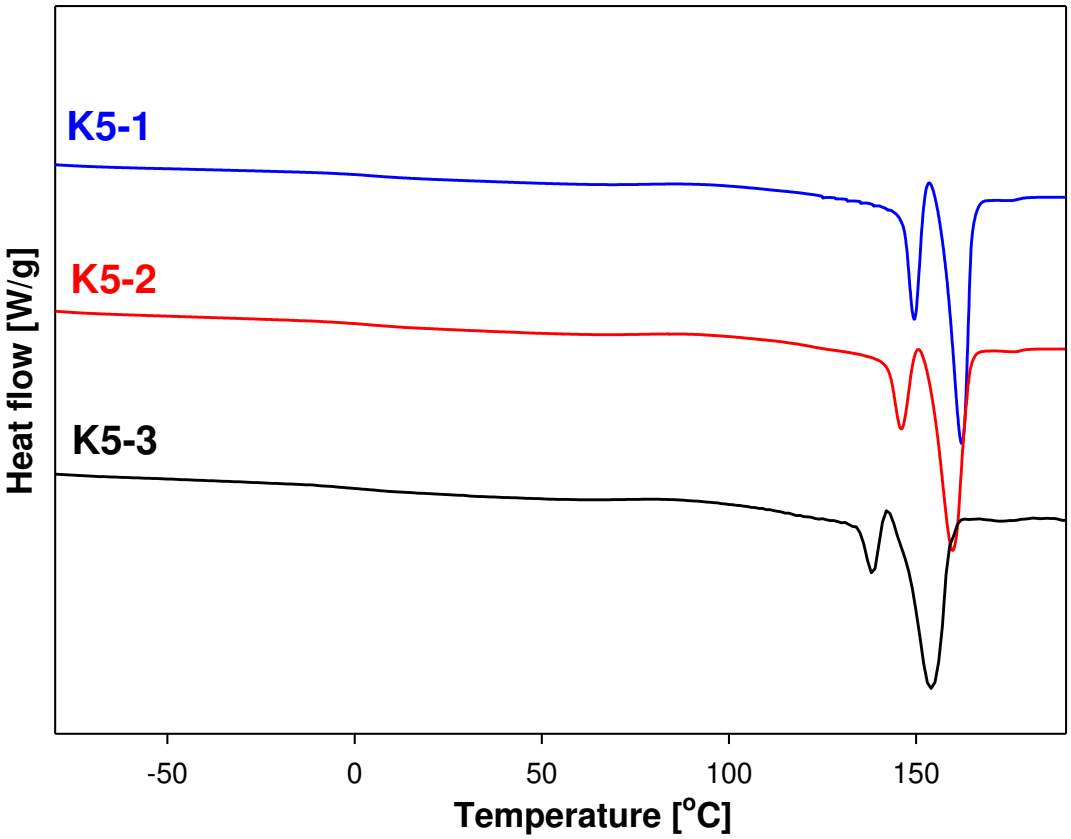

Figure 14. Comparison of heat flows of nanobiocomposites versus temperature upon heating at a rate of 10°C·min^{-1}.

The glass transition was observed in the range of 4.40°C - 5.25°C and the onset melting temperature in the range of 134.6°C - 156.7°C. The change of heat capacity and heat of fusion were also determined for future estimating the phase content of new materials. Based on Table 3 and Table 4, the lowest value of the glass transition temperature was observed for the K5-2 nanobiocomposite, which allows us to assume that this material will be the most plasticized in reference to the series of materials considered. Moreover, based on the difference between the degradation temperature and the onset melting temperature (a start of melting) processing window of nanobiocomposites was determined. The greatest processing capabilities K5-3 offers because the processing window was estimated as 122.2°C. For the remaining nanobiocomposites K5-1 and K5-2 it is 116.8°C and 118.2°C, respectively.

Table 4. Comparison of thermal parameters of nanobiocomposites upon heating their representative samples at 10°C·min^{-1} after prior cooling at the same rate.

Sample	T_g [°C]	ΔC_p [J·g^{-1}·°C^{-1}]	$T_{m\ (onset)}$ [°C]	T_{m1} [°C]	T_{m2} [°C]	ΔH_f [J·g^{-1}]	T_c [°C]	ΔH_c [J·g^{-1}]
K5-1	4.50	0.2059	156.70	149.50	162.20	90.75	86.70	68.34
K5-2	4.40	0.2328	142.00	146.00	159.80	89.78	82.87	68.97
K5-3	5.25	0.3752	134.60	138.20	153.80	85.70	77.65	63.58

4. Conclusions

New polymer blends were prepared with poly(3-hydroxybutyrate) (P3HB) and aliphatic linear polyurethane (PU). Linear polyurethane synthesized with hexamethylene 1,6-diisocyanate and butane-1,4-diol was used as modifier for P3HB in the amount of 5, 10, 15 and 20 wt.%. Thermal

stability of P3HB-PU polymer compositions was higher than that of unmodified P3HB matrix. The difference between the degradation temperature of P3HB and its polyurethane blends was 22-57°C. The difference between the melting point and degradation temperature was above 100°C for most of the polymer blends obtained. DSC analysis also showed a decrease in the glass transition temperature of the tested polymer blends. The mechanical properties of the new P3HB-PU polymer blends at 5 wt.%. modifier content showed a desirable increase in tensile strength, relative elongation at break and impact strength, and a decrease in hardness. A further increase in the PU percentage in the composition results in a deterioration of mechanical properties except for the desired decrease in hardness.

P3HB-PU polymer blends containing 5 wt.% aliphatic linear polyurethane showed the best mechanical and thermal properties, and were therefore used with different amounts of organically modified nanoclay – Cloisite®30B to prepare hybrid nanocomposites based on P3HB.

Using SAXS technique and transmission electron microscopy, it was found that polyester and polyurethane chains penetrated the interlayer spaces of organically modified montmorillonite – Cloisite 30B and complete delamination occurred during direct mixing in the extrusion process. Spectral analysis confirmed the interaction between polymers and nanofiller and their compatibility in the obtained nanobiocomposites. The morphology of the prepared hybrid nanobiocomposites demonstrated the interaction of biopolymer matrix with polyurethane and Cloisite 30B as well as the formation of polyester-polyurethane-montmorillonite adducts easily migrating in relation to each other and leading to improved mechanical properties compared to those of base P3HB and P3HB-PU polymer blends.

The incorporation of nanoplatelets into the polymer matrix ensured a better thermal stability of the hybrid nanobiocomposites. There was an increase in the onset temperature of degradation by 33°C relative to P3HB and 10°C relative to the P3HB-PU polymer blends.

The hybrid nanobiocomposites based on P3HB matrix have shown higher impact and tensile strength as well as higher relative elongation at break. The best mechanical properties were obtained by a nanobiocomposite containing 1 wt.%. Cloisite®30B (30% increase in impact strength, 11% increase in tensile strength and 58% increase in relative elongation at break). The obtained hybrid nanobiocomposites containing the smallest amount of nanofillers – 1 wt.% Cloisite®30B and 5 wt.% polyurethane were characterized by the best mechanical and thermal properties.

Author Contributions: Conceptualization, Beata Krzykowska and Iwona Zarzyka; Data curation, Beata Krzykowska, Anita Białkowska, Karol Hęclik, Lucjan Dobrowolski, Michał Longosz, Anna Czerniecka-Kubicka; Formal analysis, Iwona Zarzyka, Beata Krzykowska, Anita Biakowska, Anna Czerniecka-Kubicka; Investigation, Iwona Zarzyka, Beata Krzykowska, Anna Czerniecka-Kubicka.; Methodology, Iwona Zarzyka, Beata Krzykowska; Supervision, Iwona Zarzyka, Mohamed Bakar; Validation, Iwona Zarzyka, Anna Czerniecka-Kubicka; Visualization, Beata Krzykowska, Anna Czerniecka-Kubicka; Writing—original draft, Iwona Zarzyka, Beata Krzykowska; Writing—review and editing, Iwona Zarzyka, Beata Krzykowska, Mohamed Bakar. All authors have read and agreed to the published version of the manuscript.

References

1. Kalia, V.Ch.; Patel, S.K.S.; Shanmugam, R.; Lee, J-K. Polyhydroxyalkanoates: Trends and advances toward biotechnological applications. Bioresour. Technol. **2021**, 326, 124737.
2. Leja, K.; Lewandowicz, G. Polymer biodegradation and biodegradable polymers – A review. Polish J. Environ. Stud. **2010**, 19(2), 255–266.
3. Hablot, E.; Bordes, P.; Pollet, E.; Averous, L. Thermal and thermo-mechanical degradation of poly(3-hydroxybutyrate)-based multiphase systems. Polym. Degrad. Stabil. **2008**, 93(2), 413–421.
4. Chen, G.Q.; Wu Q. The application of polyhydroxyalkanoates as tissue engineering materials. Biomater. **2005**, 26(33), 6565-6578.
5. Ansari, S.; Sami, N.; Yasin, D.; Ahmad, N.; Fatma, T. Biomedical applications of environmental friendly poly-hydroxyalkanoates. Int. J. Biol. Macromol. **2020**, 183, 549–563.
6. Tarrahi, R.; Fathi, Z.; Özgür, M.; Seydibeyoğlu, K.; Doustkhah, E.; Khataee, A. Polyhydroxyalkanoates (PHA): From production to nanoarchitecture. Int. J. Biol. Macromol. **2020**, 146, 596–619.

7. Dias, Y. J.; Robles, J. R.; Sinha-Ray, S.; Abiade, J.; Pourdeyhimi, B.; Niemczyk-Soczynska, B.; Kolbuk, D.; Sajkiewicz, P.; Yarin, A. L. Solution-Blown Poly(hydroxybutyrate) and ε-Poly-L-lysine Submicro- and Microfiber-Based Sustainable Nonwovens with Antimicrobial Activity for Single-Use Applications. ACS Biomater. Sci. Eng. **2021**, 7(8), 3980-3992.
8. Poli, A.; Di Donato, P.;. Abbamondi, G. R.; Nicolaus, B. Synthesis, Production, and Biotechnological Applications of Exopolysaccharides and Polyhydroxyalkanoates. Archaea. **2011**, 693253, 1–13.
9. Leja, K.; Lewandowicz, G. Polymer biodegradation and biodegradable polymers – A review. Polish J. Environ. Stud. **2010**, 19(2), 255–266.
10. Sudesh, K.; Abe, H.; Doi, H. Synthesis, structure and properties of polyhydroxyalkanoates: biological polyesters. Prog. Polym. Sci. **2000**, 25(10), 1503–1555.
11. Poli, A.; Di Donato, P.; Abbamondi, G. R.; Nicolaus, B. Synthesis, Production, and Biotechnological Applications of Exopolysaccharides and Polyhydroxyalkanoates. Archaea. **2011**, 693253, 1–13.
12. Fernandes, E. G.; Pietrini, M.; Chiellini, E. Thermo-mechanical and morphological characterization of plasticized poly[(R)-3-hydroxybutyric acid]. Macrom. Symp. **2004**, 218, 157–164.
13. El-Taweel, S. H.; Höhne, G. W. H.; Mansour, A. A.; Stoll, B. Glass transition and the rigid amorphous phase in semicrystalline blends of bacterial polyhydroxybutyrate PHB with low molecular mass atactic R, S-PHB-diol. Polymer. **2004**, 45, 983–992.
14. Pan, Y.; Inoue. Polymorphism and isomorphism in biodegradable polyesters. Prog. Polym. Sci. **2009**, 34(7), 605–640.
15. Yokouchi, M.; Chatani, Y.; Tadokoro, H.; Teranishi, K.; Tani, H. Structural studies of polyesters: Molecular and crystal structures of optically active and racemic poly (β-hydroxybutyrate). Polymer. **1973**, 14(6), 267–272.
16. Lenz, R. W.; Marchessault, R. H. Bacterial Polyesters: Biosynthesis, Biodegradable Plastics and Biotechnology. Biomacromolecules. **2005**, 6(1), 1–8.
17. El-Taweel, S. H.; Höhne, G. W. H.; Mansour, A. A.; Stoll, B. Glass transition and the rigid amorphous phase in semicrystalline blends of bacterial polyhydroxybutyrate PHB with low molecular mass atactic R, S-PHB-diol. Polymer. **2004**, 45, 983–992.
18. Lee, S. N.; Lee, M.Y.; Park, W.H. Thermal stabilization of poly(3-hydroxybutyrate) by poly(glycidyl methacrylate), J. Appl. Polym. Sci. **2022**, 83, 2945–2952.
19. Khanna, S.; Srivastava, A. K. Recent advances in microbial polyhydroxyalkanoates. Process. Biochem. **2005**, 40, 607-619.
20. Palmeiro-Sánchez, T.; O'Flaherty, V.; N.L. Lens, P. Polyhydroxyalkanoate bio-production and its rise as biomaterial of the future. J. Biotechnol. **2022**, 348, 10-25.
21. Ribeiro, P. L. L.; Figueiredo, T. V. B.; Moura, L. E.; Druzian, J. I. Chemical modification of cellulosevnanocrystals and their application in thermoplastic starch (TPS) and poly(3-hydroxybutyrate) (P3HB) nanocomposites. Polym Adv Technol. **2019**, 30, 573–583.
22. Chieng, BW.; Ibrahim, NA.; Then, YY.; Loo, YY. Epoxidized Vegetable Oils Plasticized Poly(lactic acid) Biocomposites: Mechanical, Thermal and Morphology Properties. Mol. **2014**, 19, 16024–16038.
23. Garcia-Garcia, D.; Ferri, J.M.; Montanes, N.; Lopez-Martinez, J.; Balart, R. Plasticization effects of epoxidized vegetable oils on mechanical properties of poly(3-hydroxybutyrate). Polym Int. **2016**, 65, 1157–1164.
24. Al-Mulla, EAJ.; Yunus, WMZW.; Ibrahim, NAB .; Ab Rahman, MZ. Physical properties of plasticized PLA/HNTs bionanocomposites: effects of plasticizer type and content. JMater Sci. **2010**, 45, 1942–1946.
25. Zhao, Y.; Qu, J.; Feng, Y.; Wu, Z.; Chen, F.; Tang ,H. Mechanical and thermal properties of epoxideized soybean oil plasticized polybutylene succinate blends Polym Adv Technol. **2012**, 23, 632–638.
26. Seydibeyoglu, MO. ; Misra, M.; Mohanty, A. Progress in bio-based plastics and plasticizing modifications. Int J Plast Technol. **2010**, 14, 1–16.
27. Ferri, JM.; Samper, M.; Garcia-Sanoguera, D.; Reig, M.; Fenollar, O.; Balart, R. Plasticizing effect of biobased epoxidized fatty acid esters on mechanical and thermal properties of poly(lactic acid). JMater Sci. **2016**, 51, 5356–5366.
28. Jost, V.; Kopitzky, R. Blending of Polyhydroxybutyrate-co-valerate with Polylactic Acid for Packaging Applications – Reflections on Miscibility and Effects on the Mechanical and Barrier Properties. Chem Biochem Eng Q. **2015**, 29, 221–246.
29. Wang, W.; Zhu, X.; Wang, X.; Chen, G.Q.; Chen, K.Xu. Processability modifications of poly (3-hydroxybutyrate) by plasticizing, blending, and stabilizing, J. Appl. Polym.Sci. **2008**, 107 (1), 166–173.
30. Ali, F.; Chang, Y-W.; Kang, SC.; Yoon, JY. Thermal, mechanical and rheological properties of poly (lactic acid)/epoxidized soybean oil blends. Polym Bull. **2009**, 62, 91–98.
31. Silverajah, VSG.; Ibrahimm, NA.; Zainuddin, N.; Yunus, WMZW.; Abu Hassan, H. Mechanical, Thermal and Morphological Properties of Poly(lactic acid)/Epoxidized Palm Olein Blend. Mol. **2012**, 17, 11729–11747.

32. Al-Mulla, EAJ.; Yunus, WMZW.; Ibrahim, NAB.; Ab Rahman, MZ. Properties of epoxidized palm oil plasticized polytlactic acid. JMater Sci. **2010**, 45, 1942–1946.
33. Silverajah, VSG.; Ibrahim, NA.; Yunus WMZW.; Abu Hassan, H.; Woei, CB. Thermal and Morphological Characterization of Poly(lactic acid)/Epoxidized Palm Oil Blend. Int J Mol Sci. **2012**, 13, 5878–5898.
34. Prempeh, N.; Li, J.; Liu, D.; Das, K.; Maiti, S.; Zhang, Y. Plasticizing effects of epoxidized sun flower oil on biodegradable polylactide films: A comparative study. Polym Sci Ser A. **2014**, 56, 856–863.
35. 35. Fernández-Ronco, M.P.; Gradzik, B.; Gooneie, A.; Hufenus, R.; El Fray, M. Tuning poly(3 hydroxybutyrate) (P3HB) properties by tailored segmented bio copolymers. ACS Sustainable Chem. Eng. **2017**, 5, 11060-11068.
36. Kozlowska, A.; Gromadzki, D.; El Fray, M.; S˘te˘pánek, P. Morphology evaluation of biodegradable copolyesters based on dimerized fatty acid studied by DSC, SAXS and WAXS. Fibres TextEastEur. **2008**, 16, 85.
37. Mirmusavi, M.H. Assessing the physical and mechanical properties of poly 3-hydroxybutyrate-chitosan-multi-walled carbon nanotube/silk nano–micro composite scaffold for long-term healing tissue engineering applications. Micro Nano Lett. 13. **2018**, 829–834.
38. Zarei, M.; Karbasi, S. Evaluation of the effects of multiwalled carbon nanotubes on electrospun poly (3-hydroxybutirate) scaffold for tissue engineering applications. J. Porous Mat. 25. **2018**, 259–272.
39. Barud, HS,; Souza, JL. Bacterial cellulose/ poly(3-hydroxybutyrate) composite membranes. Carbohydr Polym Santos DB. **2011**, 83, 1279–1284.
40. Thiré, RMSM.; Ribeiro, TAA.; Andrade, CT. Efect of starch addition on compression-molded poly(3-hydroxybutyrate)/starch blends. J Appl Polym Sci. **2006**, 100, 4338–4347.
41. Dos Santos, BR.; Bacalhau, FB.; Pereira, TDS. Chitosan-montmorillonite microspheres: a sustainable fertilizer delivery system. Carbohydr Polym. **2015**, 127, 340–346.
42. Souza, J. L.; de Campos, A.; França, D.; Faez, R. PHB and montmorillonite clay composites as KNO3 and NPK support for a controlled release. J Polym Environ. **2019**, 27, 2089–2097.
43. Isa, M. R. M.; Hassan, A.; Nordin, N. A.; Thirmizir, M. Z. A.; Ishak, Z. A. M. Mechanical, rheological and thermal properties of montmorillonite-modified polyhydroxybutyrate composites. High Perform. Polym. **2020**, 32(2), 192–200.
44. D'Amico, DA.; Manfredi, LB.; Cyras, VP. Relationship between thermal properties, morphology, and crystallinity of nanocomposites based on polyhydroxybutyrate. J Appl Polym Sci. **2012**, 123, 200–208.
45. Joshi, S. Can nanotechnology improve the sustainability of biobased products? The case of layered silicate biopolymer nanocomposites. J Ind Ecol. **2014**, 12, 474–489.
46. Yan, XU.; Zhou, Wanru.; Ma, Xiaojun.; Sun, Binqing. Fabrication and characterization of poly(3-hydroxybutyrate-co3-hydroxyhexanoate) modified with nano-montmorillonite biocomposite, e-Polymers. **2021**, 21, 38–46.
47. Hussain, F.; Hojjati, M.; Okamoto, M. Polymer-matrix nanocomposites, processing, manufacturing, and application. J Compos Mater. **2006**, 40, 1511–1575.
48. Li, DN.; Fu, JR.; Ma, XJ. Improvement in thermal, mechanical, and barrier properties of biocomposite of poly(3-hydroxybutyrateco-3-hydroxyhexanoate)/modified nano-SiO2. Polym Compos. **2020**, 41(1), 381–390.
49. Risyon, NP.; Othman, SH.; Basha ,RK.; Talib, RA. Effect of halloysite nanoclay concentration and addition of glycerol on mechanical properties of bionanocomposite films. Polym Polym Compos. **2016**, 24, 795–801.
50. Souza, AC.; Goto, GEO.; Mainardi, JA.; Coelho, ACV.; Tadini, CC. Cassava starch composite films incorporated with cinnamon essential oil: antimicrobial activity, microstructure, mechanical and barrier properties. LWT-Food Sci Technol. **2013**, 54(2), 346–52.
51. Jandas, P. J.; Prabakaran, K.; Kumar, R.; Mohanty, S.; Nayak, S. K. Eco-friendly poly (hydroxybutyrate) nanocomposites: preparation and characterization. J. Polym. Res. **2021**, 28, 285.
52. D'Amico, DA.; Manfredi, LB.; Cyras, VP. Relationship between thermal properties, morphology, and crystallinity of nanocomposites based on polyhydroxybutyrate. JAppl Polym Sci. **2012**, 123(1), 200–208.
53. Botana, A.; Mollo, M.; Eisenberg, P.; Torres Sanchez, R. M.; Effect of modified montmorillonite on biodegradable PHB nanocomposites. Appl Clay Scie. **2010**, 47, 263–270.
54. Utracki, A.L.; Jamieson, A.M. Polymer Physics: From Suspensions to Nanocomposites and Beyond. Wiley: Hoboken. **2010**,
55. Thiré, R.M.; Arruda, L.C.; Barreto, L.S. Morphology and thermal properties of poly(3-hydroxybutyrate-co-3-hydroxyvalerate)/attapulgite nanocomposites. Mater. Res. **2011**, 14, 340–344.